

## Film Thickness Effect on Properties of Co-ZnO Thin Films Prepared by Sol-Gel Method

M. Medjalidi<sup>1,\*</sup>, N. Dadda<sup>2</sup>, A.R. Khantoul<sup>3</sup>, I. Ameer<sup>4</sup>, A. Kassaa<sup>3</sup>, A. Boumaiza<sup>4</sup>,  
B. Boudine<sup>4</sup>, M. Sebais<sup>4</sup>

<sup>1</sup> Laboratory of SATIT, University Abbes Laghrour Khenchela, Algeria

<sup>2</sup> Laboratoire de Synthèse et Biocatalyse Organique (LSBO), Département de Chimie,  
Université Badji Mokhtar Annaba, B.P. 12, 23000 Annaba, Algeria

<sup>3</sup> Research Center in Industrial Technologies CRTI, P. O. Box 64, Cheraga 16014 Algiers, Algeria

<sup>4</sup> Crystallography Laboratory, Physics Department, Faculty of Exact Sciences,  
Mentouri Brothers- Constantine 1 University, Route Ain El Bey, 25000 Constantine, Algeria

(Received 01 November 2022; revised manuscript received 22 December 2022; published online 27 December 2022)

1 wt. % Co-doped ZnO (CZO) thin films of varying thicknesses (3, 5 and 7 layers, which correspond to 403, 545 and 725 nm as thickness) are deposited using the sol-gel method onto glass substrates by dip coating technique. Zinc acetate dehydrate, cobalt acetate, 2-methoxyethanol and ethanolamine are used as primary materials, solvent and stabilizer, respectively. The thermally annealed films are characterized to study the structural, surface morphology, electrical and optical properties. X-ray diffraction (XRD) shows that these films have a polycrystalline hexagonal structure (wurtzite structure with space group P63mc), possessing compressive stress and presenting a preferred orientation along the (002) plane. We note that the particle size increases when the thickness increases. The surface morphology of the prepared CZO thin films is investigated by atomic force microscopy (AFM). It reveals the emergence of a uniform columnar structure and shows that the particle size and the root mean square (RMS) of CZO increase with increasing thickness. UV-visible spectroscopy shows (in the visible region) a transmittance between 75 and 86 % for all the films, strong absorption (in the UV region) and a decrease in the optical band gap. Moreover, the near band edge (NBE) and visible emissions detected by photoluminescence are affected by the thickness. The electrical conductivity of the sample with 725 nm is found to be  $4.43 (\Omega\text{-cm})^{-1}$ .

**Keywords:** Co-doped ZnO thin films, Dip-coating, Thickness, Photoluminescence, XRD, Electrical conductivity.

DOI: [10.21272/jnep.14\(6\).06023](https://doi.org/10.21272/jnep.14(6).06023)

PACS numbers: 81.20.Fw, 68.55.ag, 68.55.jd,  
68.55.J\_, 78.68.\_m

### 1. INTRODUCTION

Recently, zinc oxide (ZnO) has been widely exploited in solar cells, light-emitting electrode tubes, UV detectors, lasers, surface acoustic wave devices, transparent bright conduction electrodes, spintronic devices, nanobiosensors designs, optoelectronic and gas sensors [1-4]. It has a wide range of applications, which has increased people's interest in its optical and electrical properties. ZnO is a direct band gap semiconductor ( $E_g = 3.37$  eV). It has a high exciton binding energy (60 meV) at room temperature [5]. There are many preparation methods for ZnO thin films, such as pulsed laser deposition [6], colloidal [7], chemical vapor deposition (CVD) [8], coprecipitation method [9], RF magnetron sputtering [10], sol-gel [11], spray pyrolysis [12], etc.

The properties of ZnO thin films prepared depend on the process parameters used in processing. Although there are several reports regarding the effect of different parameters of elaboration methods, however, the influence of the thickness on the characteristics of ZnO films has not been widely reported. Myoung et al. [6] reported that the structural, electrical and optical properties of ZnO films grown by pulsed laser deposition on sapphire (0001) substrates are thickness dependent. Reddy et al. [10] studied the effect of film thickness on the structural, morphological and optical properties of ZnO films prepared by RF magnetron sputtering. Kumar et al. [11]

presented the effect of thickness variation on the structural, morphological and optical properties of ZnO films deposited on glass substrates by the sol-gel spin coating technique. For application in optoelectronic devices, the optimum film thickness is normally chosen to obtain the best device performance. With this in mind, it is very important to study the effect of film thickness on the properties of ZnO films. Therefore, Co-doped ZnO thin films of different thicknesses were prepared by the sol-gel method on glass substrates via the dip-coating technique. The impact of the thickness on the structural, morphological, optical and electrical properties of ZnO films has been studied.

### 2. EXPERIMENTAL DETAILS

0.7 g of zinc acetate dihydrate ( $\text{Zn}(\text{AC})_2$ ) was dissolved in 30 ml of 2-methoxyethanol at room temperature. When the solution turned milky, 0.6 ml of monoethanolamine (MEA) was added drop by drop in the above solution. After stirring at 60 °C for 1 h, we obtained a clear, transparent and homogeneous solution. The presence of OH in 2-methoxyethanol contributes to the conversion of salt to a hydroxide by thermal decomposition. Co doping solution was prepared by dissolving X (g) in 30 ml of the pure solution to get a rate mass doping of 1 wt. %. After stirring at 60 °C for 15 min, the solution became homogeneous. The doping solution was

\* [malika.medjalidi@univ-khenchela.dz](mailto:malika.medjalidi@univ-khenchela.dz)

† [med\\_malika@yahoo.fr](mailto:med_malika@yahoo.fr)

then deposited by dip coating technique on cleaned glass substrate using the dipping speed controller at 10 mm/h. The preheated temperature of the thin films is taken at 350 °C for 15 min.

Meanwhile, the evaporation of the solvent occurred, while the heat treatment was carried out at 500 °C for 2 h in order to promote the thermal decomposition of zinc hydroxide and the crystallization of ZnO.

The crystalline structure was analyzed with X-ray diffraction (XRD), the data presented in this work were obtained using a PANalytical X'Pert Pro Philips diffractometer (with Cu-K $\alpha$  radiation source; wavelength  $\lambda = 1.5406 \text{ \AA}$ , and a Ni filter at 40 kV and 20 mA in the  $2\theta$  range (10-80°). The morphology was identified by using Atomic Force Microscopy (AFM) through a nano-observer atomic force microscope developed by CS Instruments. The UV-visible spectra of ZnO thin films were characterized by an UV-Vis Shimadzu double-beam spectrophotometer in the energy region of 2-6 eV, (UV-3101 PC) in the wavelength range 300-900 nm. The PL spectra measurements were carried out using a 380 nm lamp excitation from a Perkin-Elmer LS 50B luminescence spectrophotometer. The film thickness was measured using surface-profilometry.

### 3. RESULTS AND DISCUSSION

#### 3.1 Structural Properties

Fig. 1 shows the relationship between the CZO film thickness and the number of coatings. It can clearly be seen that the film thickness depends quasi-linearly on the number of coatings. Such dependence represents a typical characteristic of the sol-gel dip-coating method, and the average film per coating cycle is estimated to be approximately 115 nm.

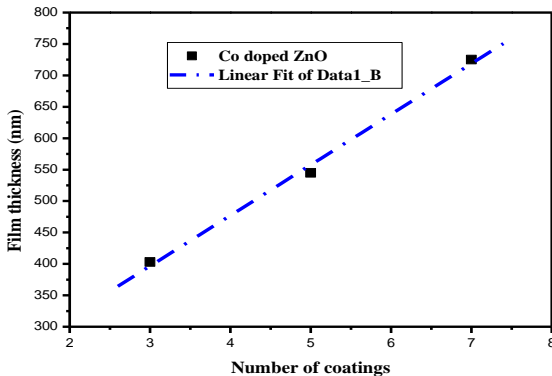


**Fig. 1** – Thickness of Co-doped ZnO films as a function of the number of coatings. The dashed line represents linear fit to the experimental data

To investigate the thickness effect on the crystalline quality of the CZO films, XRD analysis was performed. Fig. 2 displays the XRD spectra of all the CZO thin films deposited on the glass substrate at various thicknesses recorded in the  $2\theta$  diffraction range 10-80°. It can be seen that three diffraction peaks were recorded for  $2\theta$  diffraction angles of 31.7, 34.4 and 36.2° corresponding to the (100), (002) and (101) peaks respectively.

All diffraction peaks ((100), (002) and (101)) were indexed with the hexagonal wurtzite crystal structure of ZnO (JCPDS card no. 36-1451) [3], and it is seen that

in all the films the peak, associated with the (002) plane, is predominant regardless of the film thickness. As previously reported in the literature, the  $c$  axis preferential orientation may be associated with the minimization of the surface energy and internal stress, as well as the highest atomic density found along the (002) plane [5].

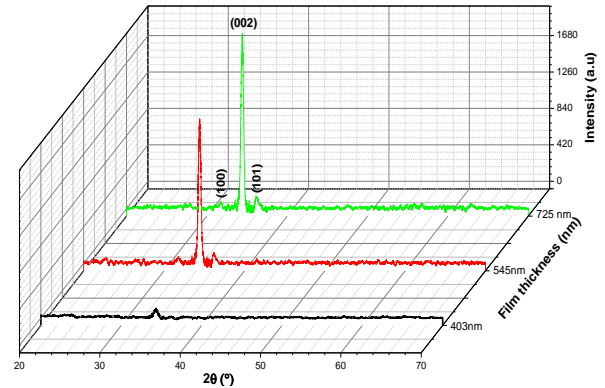


**Fig. 2** – XRD spectra of Co-doped ZnO thin films with different thicknesses after the thermal treatment at 500 °C for 1 h

As the film thickness increases, the (002) peak becomes intense and sharper, indicating an improvement in the crystal quality of the films. Despite the existence of very weak additional peaks associated with the (100) and (101) planes of the hexagonal phase in CZO films with a thickness exceeding 403 nm, the increase in the film thickness mainly affected the intensity of the preferred orientation (002) in thin films.

An increase in intensity can be a direct consequence of an increase in film thickness. This result is in good agreement with that already found by the authors of references [2].

The crystallite size  $D$  (nm) of CZO films was determined using the Scherrer formula [11]:

$$D = \frac{k\lambda}{\beta \cos \theta}, \quad (1)$$

where  $k$  is a constant known as the shape factor value equal to 0.9,  $\lambda$  is the wavelength of the Cu-K $\alpha$  line ( $\lambda = 0.15406 \text{ nm}$ ),  $\beta$  is the full width at half maximum (FWHM) of the diffraction peak measured in radians, and  $2\theta$  is the Bragg diffraction angle. The calculated values of  $D$  are listed in Table 1. The average sizes of ZnO crystallites are found to be 14.8, 20.7 and 22.9 nm for 403, 545 and 725 nm CZO thin films respectively. Thicker films exhibit larger crystallite size.

We noticed that all samples have nanometric crystallite sizes. This result is in good agreement with literature data [13, 14].

The lattice constants for the ZnO hexagonal structure have been calculated using Bragg's law:

$$2d_{hkl} \sin \theta_{hkl} = n\lambda, \quad (2)$$

where  $d_{hkl}$  is the inter-planar spacing,  $\theta$  is the Bragg diffraction angle,  $n$  is the diffraction order ( $n = 1$ ), and  $\lambda$  is the Cu-K $\alpha$  radiation wavelength.

Also, we can find that the  $d_{hkl}$  of the hexagonal lattice can be written as [13]:

$$\frac{1}{d_{hkl}^2} = \frac{4}{3} \left( \frac{h^2 + k^2 + hk}{a^2} \right) + \left( \frac{l^2}{c^2} \right), \quad (3)$$

where  $h$ ,  $k$  and  $l$  represent the Miller indices of the planes,  $a$  and  $c$  are the lattice parameters.

For the (002) peak, the lattice constant  $c$  was calculated with  $c = 2d_{002}$ . The values of the lattice constant  $c$  were found to be 5.2254, 5.2041 and 5.2080 Å for 403, 545, 725 nm, respectively. Then the lattice parameter  $a$  can be calculated for (100) peak with  $a = 2d/\sqrt{3}$ . It is noted that the lattice parameter  $a$  increases from 3.2205 to 3.2564 nm with increasing thickness. The variations of the lattice parameters are shown in Table 1.

The dislocation density  $\delta$  is defined as the length of dislocation lines per unit volume (lines/nm<sup>2</sup>). The dislocation density  $\delta$  of ZnO films is calculated by the following equation [13]:

$$\delta = \frac{1}{D^2} \quad (4)$$

The residual in-plane stress  $\sigma$  (GPa) of the films was calculated using the following relations [11]:

$$\sigma = 2C_{13} - \frac{(C_{11} + C_{12})C_{33}^{film}}{C_{13}} e_{zz} \quad (5)$$

$$C_{33}^{film} = \frac{0.99C_{33}^{crystal}}{(1 - e_{zz})^4}, \quad (6)$$

$$e_{zz} = \left( \frac{c - c_0}{c_0} \right) 100\% \quad (7)$$

where  $C_{ij}$  are the elastic constants of ZnO, taking the following values:  $C_{11} = 209.7$  GPa,  $C_{12} = 121.1$  GPa,  $C_{13} = 105.1$  GPa,  $C_{33} = 210.9$  GPa. And the lattice parameter of JCPDS card is  $C_0 = 5.1876$  Å. The data from XRD analysis including  $2\theta$  angle,  $hkl$  plane,  $d$ -spacing, FWHM, lattice parameters values,  $ca$  ratio and crystallite size are shown in Table 1.

**Table 1** – Values of the calculated parameters and lattice stresses of CZO thin films with different thicknesses grown on glass substrates

Sample	$d = 403$ (nm)	$d = 545$ (nm)				$d = 725$ (nm)		
$2\theta$ (°)	34.281	31.762	34.425	36.269	31.703	34.400	36.254	
FWHM (°)	0.561	0.514	0.385	0.440	0.277	0.376	0.469	
( $hkl$ )	(002)	(100)	(002)	(101)	(100)	(002)	(101)	
$d_{hkl}$ (Å)	2.61268	2.81509	2.60206	2.47487	2.82011	2.60399	2.47586	
$D_{moy}$ (nm)	14.8	20.7				22.9		
$a$ (Å)	–	3.2505				3.2564		
$c$ (Å)	5.2254	5.2041				5.2080		
$c/a$	–	1.60				1.60		
$\delta \cdot 10^{-4}$ (lines/nm <sup>2</sup> )	45.65	23.33				19.07		
$e_{zz}$	–0.00730	–0.00318				–0.00393		
$C_{33}^{(film)}$	202.804	206.156				205.541		
$\sigma$ (GPa)	1.6	1.4				1.7		

As shown in Table 1, the FWHM decreases from 0.561 to 0.376°. Consequently, the average size of the crystallite increases from 14.8 to 22.9 nm when the film thickness varies from 403 to 725 nm. This observation suggests that crystallite sizes increase in the same manner as crystallinity, indicating that the structural properties of CZO films improve with rising film thickness.

### 3.2 Morphological Properties

It is noteworthy to investigate the effect of CZO films with different thickness on the surface morphology, which may affect the properties of the devices. AFM images of  $10 \times 10 \mu\text{m}^2$  scan areas on the films were taken in non-contact mode.

Two and three-dimensional AFM images of the surface morphology are displayed in Fig. 3 for 403, 545 and 725 nm of CZO thin films, respectively.

All CZO films show homogenous grain distribution characterized by columnar growth perpendicular to the substrate. This observation is in agreement with the XRD results ( $c$ -axis orientation). Furthermore, the films exhibit different surface topographies, which seems to be dependent on the film thickness. The root mean square roughness (RMS) and  $R_a$  were deduced from these images and their values are shown in Table 2. Based on the data analysis, the RMS values vary between 5.36 and 32.44 nm when the film thickness varies between 403 and 725 nm, indicating that the films are very smooth.

This observation of increasing RMS is mainly attributed to the columnar growth related to the  $c$ -axis texture/growth with thickness.

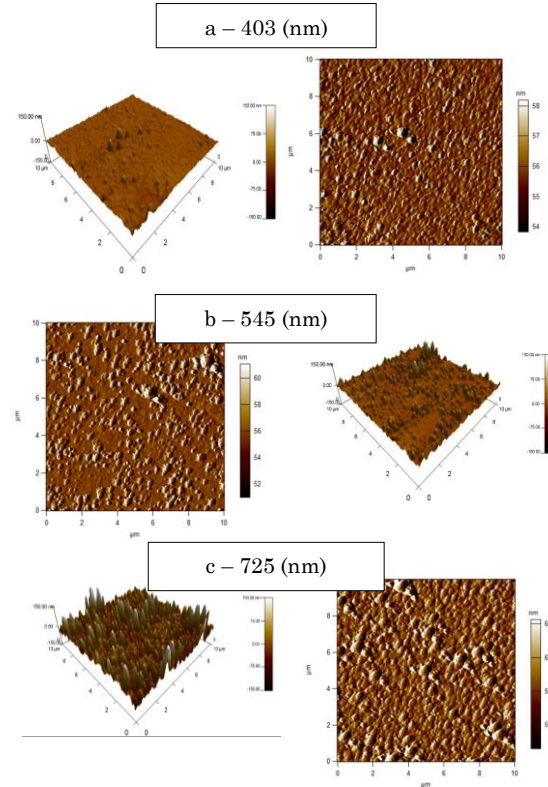


**Fig. 3** – AFM micrographs of CZO thin films with different thicknesses: (a) 403 nm, (b) 545 nm, (c) 725 nm

**Table 2** – AFM results with parameters for the CZO thin films

Samples thicknesses (nm)	RMS roughness, (nm)	Average roughness, $R_a$ (nm)
403	5.36	3.43
545	13.46	9.27
725	32.44	23.43

### 3.3 Optical Properties

The fundamental optical properties of the investigated CZO films were studied by spectral transmittance. The optical measurements of transmittance for CZO samples of different film thicknesses are shown in Fig. 4.

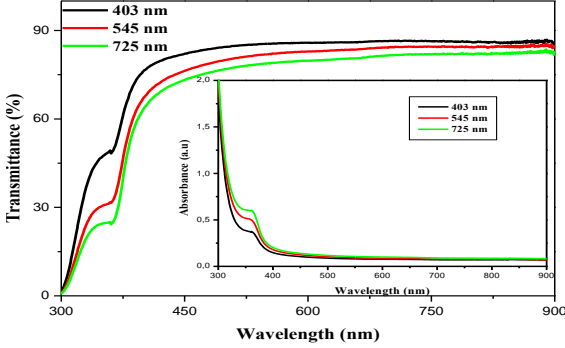


**Fig. 4** – Optical transmittance spectra of zinc oxide thin films of different thicknesses (the inset corresponds to optical absorption of CZO thin films) on glass substrate after annealing at 500 °C

The measurements have been taken in the wavelength range 300-900 nm. We note the presence of a region of high transparency between 380 and 900 nm with a maximum transmittance (about 86%) for the film with 407 nm thickness. The film of 729 nm is relatively less transparent with transmission of about 81 % at 900 nm. A similar behavior was observed by Necib et al. for Al-doped ZnO prepared by sol-gel [4]. This decrease in transmittance with film thickness may be attributed to the thickness effect along with morphological changes and higher reflection loss due to roughness induced surface scattering in the films [9]. On the other hand, the region of strong absorption (the near-UV) corresponds to the fundamental absorption ( $\lambda < 380$  nm) in CZO films.

All CZO films exhibit a sharp absorption edge in the UV range due to the direct transition of electrons between the valence band and the conduction band. As seen from the inset of Fig. 4, the absorption edge of the samples shifts towards longer wavelengths with increasing thickness, indicating that an increase in the film thickness leads to a decrease in the optical band gap.

Based on the transmittance spectra in Fig. 4, the optical band gap  $E_g$  was obtained by extrapolating the linear portion of the  $(ah\nu)^2$  versus  $(h\nu)$  plot to  $\alpha = 0$  (Fig. 5) according to the following equation [10]:

$$ah \equiv \beta (h - E_g)^n \quad (8)$$

where  $\alpha$  is the absorption coefficient of the films; it was calculated from the transmittance using the equation  $\alpha = (-1/d) \ln T$ , where  $T$  is the transmittance and  $d$  is the film thickness;  $\beta$  is the constant,  $h\nu$  is the energy of photons,  $\nu$  is the photon frequency,  $n$  has different values depending on the optical absorption process (ZnO is one of the most important multifunctional  $n$ -type direct band gap semiconductors, so it was found that for ZnO  $n = 1/2$  is the best fit),  $E_g$  is the optical band gap.

The band gap values obtained from CZO films are summarized in Table 3. These values are close to the

values of the optical gap of CZO reported by Benramache et al. [12].

The Urbach tail is the exponential region in the absorption spectrum, which is a function of the absorption coefficient and photon energy. It reveals shifts between the tails of the conduction and valence bands. We have used the Urbach energy (Table 3), which is related to the disorder in the film network, expressed as follows [12]:

$$\alpha = \bar{\alpha}_0 \exp\left(\frac{h\nu}{E_u}\right) \quad (9)$$

The Urbach energy of the CZO thin films have been estimated from the slopes of  $\ln(\alpha)$  versus photon energy ( $h\nu$ ) plots (see Fig. 6). The inverted slope of  $\ln(\alpha)$  versus photon energy ( $h\nu$ ) plot determines the values of the Urbach energy (see Table 3).

**Table 3** – Values of the optical gap and Urbach energy of CZO thin films of different thicknesses

Thicknesses (nm)	$E_g$ (eV)	Urbach energy (meV)
403	3.53	351
545	3.41	346
725	3.20	337

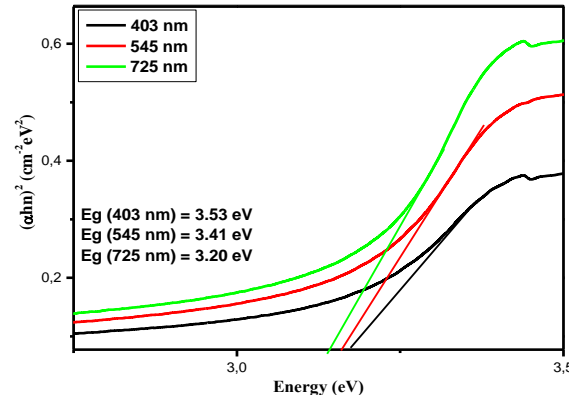


**Fig. 5** – Variation of  $(ah\nu)^2$  as a function of energy for Co-doped ZnO samples of different thicknesses

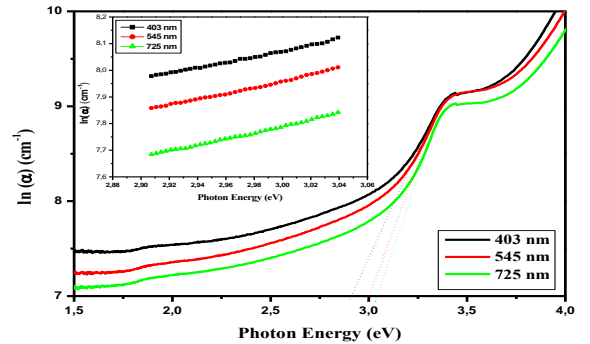


**Fig. 6** – Variations of the energy gap and Urbach energy (the inset) at different thicknesses

The values of Urbach energy ( $E_u$ ) are calculated by taking the reciprocal of the slope of the linear part in the lower photon energy region of these curves. The estimated Urbach energy of CZO films is found to decrease from 351 to 337 meV with increasing film thickness (Table 3). The variation in Urbach energy in deposited films may be due to the decrease in the grain



boundaries. We note that  $E_g$  and  $E_u$  decrease when the film thickness increases.

### 3.4 Photoluminescence (PL) Analysis

The room temperature luminescence spectra of our thin films were recorded in the 440-540 nm range under Xenon lamp excitation ( $\lambda_{exc} = 380$  nm). Fig. 7 shows the photoluminescence (PL) spectra of CZO thin films. It seems quite obvious that the intensity of the spectra changes with a very significant rate with increasing thickness (408, 523 and 729 nm). The PL spectra have four peaks originating around 446 nm (2.78 eV), 467 nm (2.65 eV), 478 nm (2.59 eV) and 515 nm (2.40 eV) [5, 13], which correspond to the violet-blue, blue, blue-green and green emission (515 nm) respectively. It is clear from the figure, those overall intensities of all the peaks increase with increasing thickness (408, 523 and 729 nm).

The blue emission peak at 467 nm is attributed to the transition of electrons from the donor level of singly ionized oxygen vacancies to the valence band [13]. We found that the emission intensity of our samples increases as the thickness increases.

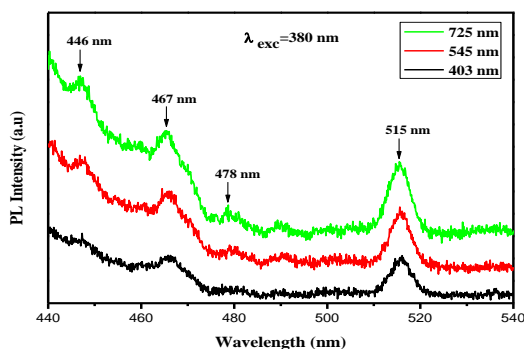


Fig. 7 – PL spectra of CZO films with different thicknesses

### 3.5 Electrical Properties

Fig. 8 shows the variation of the electrical conductivity of different thickness for CZO thin films. It is noted that the conductivity of the samples has increased from  $2.57 (\Omega \text{ cm})^{-1}$  to  $4.43 (\Omega \text{ cm})^{-1}$  with increasing thickness from 403 to 725 nm. The obtained

results reveal that the conductivity of the samples is dependent on crystallinity, as shown by the XRD results and an increase in the grain size.

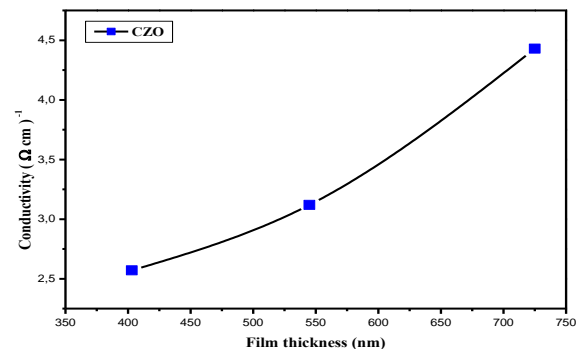


Fig. 8 – Variation of the electrical resistivity as a function of the film thickness for ZnO:Co thin films

## 4. CONCLUSIONS

The properties of CZO thin films with different thickness prepared by sol-gel dip-coating technique were investigated. XRD analysis confirmed that the ZnO thin films have a hexagonal (wurtzite) structure with a preferential orientation (002) along the  $c$ -axis perpendicular to the substrate. The crystallites forming all our layers have nanometric sizes and increase with increasing film thickness. The AFM images indicate that the RMS and  $R_q$  of CZO thin films increase with increasing film thickness, these results are in good agreement with XRD analysis. The optical transmittance of all the films is between 75 and 86 % in the visible range. The optical band gap and Urbach energy values of CZO thin films increase with film thickness. Room temperature PL measurements display NBE emissions, followed by defect-related emission peaks in the visible range.

## ACKNOWLEDGEMENTS

The authors would like to thank Prof. M. Diaf and Dr. H. Boubekri from the Laboratory of Laser Physics, Optical Spectroscopy and Optoelectronics (LAPLASO), Badji Mokhtar Annaba University, Algeria, for the photoluminescence analysis.

## REFERENCES

1. S. Fay, J. Steinhauser, N. Oliveira, E. Vallat-Sauvain, C. Ballif, *Thin Solid Films* **515**, 8558 (2007).
2. V. Musat, A.M. Rego, R. Monteiro, E. Fortunato, *Thin Solid Films* **516**, 1512 (2008).
3. Y. Meng, Y. Lin, J. Yang, *Appl. Surf. Sci.* **268**, 561 (2013).
4. K. Necib, T. Touam, A. Chelouche, L. Ouarez, D. Djouadi, B. Boudine, *J. Alloy. Compd.* **735**, 2236 (2018).
5. M. Medjaldi, O. Touil, B. Boudine, M. Zaabat, O. Halimi, M. Sebais, L. Ozyuzer, *Silicon* **10**, 2577 (2018).
6. J.M. Myoung, W.H. Yoon, D.H. Lee, I. Yun, S.H. Bae, S.Y. Lee, *Jpn. J. Appl. Phys.* **41**, 28 (2002).
7. A. Singhal, S.N. Achary, A.K. Tyagi, P.K. Manna, S.M. Yusuf, *Mater. Sci. Eng. B* **153**, 47 (2008).
8. K. Maejima, T. Koida, H. Sai, *Thin Solid Films* **559**, 83 (2014).
9. J. Xu, Z. Yang, H. Wang, X. Zhang, *Bull. Mater. Sci.* **37**, 895 (2014).
10. R.S. Reddy, A. Sreedhar, A.S. Reddy, S. Uthanna, *Adv. Mater. Lett.* **3**, 239 (2012).
11. V. Kumar, N. Singh, R.M. Mehra, A. Kapoor, L.P. Purohit, H.C. Swart, *Thin Solid Films* **539**, 161 (2013).
12. S. Benramache, B. Benhaoua, H. Bentrach, *J. Nanostruct. Chem.* **3**, 54 (2013).
13. B. Rahal, B. Boudine, Y. Larbah, M. Siad, N. Souami, *J. Inorg. Organomet. Polym. Mater.* **31**, 4001 (2021).
14. A.R. Khantoul, M. Sebais, B. Rahal, B. Boudine, O. Halimi, *Acta Phys. Pol. A* **133**, 114 (2018).

**Вплив товщини плівки на властивості тонких плівок Co-ZnO,  
отриманих золь-гель методом**

M. MedjalDI<sup>1</sup>, N. Dadda<sup>2</sup>, A.R. Khantoul<sup>3</sup>, I. Ameur<sup>4</sup>, A. Kassaa<sup>3</sup>, A. Boumaiza<sup>4</sup>,  
B. Boudine<sup>4</sup>, M. Sebais<sup>4</sup>

<sup>1</sup> *Laboratory of SATIT, University Abbes Laghrour Khenchela, Algeria*

<sup>2</sup> *Laboratoire de Synthèse et Biocatalyse Organique (LSBO), Département de Chimie,  
Université Badji Mokhtar Annaba, B.P. 12, 23000 Annaba, Algeria*

<sup>3</sup> *Research Center in Industrial Technologies CRTI, P. O. Box 64, Cheraga 16014 Algiers, Algeria*

<sup>4</sup> *Crystallography Laboratory, Physics Department, Faculty of Exact Sciences,  
Mentouri Brothers- Constantine 1 University, Route Ain El Bey, 25000 Constantine, Algeria*

Тонкі плівки ZnO, леговані 1 мас. % Co (CZO) різної товщини (3, 5 і 7 шарів, що відповідають товщині 403, 545 і 725 нм) наносяться золь-гель методом на скляні підкладки технікою нанесення покриттів зануренням. Дегідрат ацетату цинку, ацетат кобальту, 2-метоксиетанол і етаноламін використовуються відповідно як первинні матеріали, розчинник і стабілізатор. Термічно відпалені плівки охарактеризовано для вивчення структури, морфології поверхні, електричних та оптичних властивостей. Дифракція рентгенівських променів (XRD) показує, що ці плівки мають полікристалічну гексагональну структуру (структура вюрциту з просторовою групою P63mc), володіють напруженою стиску та мають переважну орієнтацію вздовж площини (002). Відзначимо, що при збільшенні товщини розмір частинок зменшується. Морфологію поверхні отриманих тонких плівок CZO досліджують за допомогою атомно-силової мікроскопії (AFM). Вона виявляє появу однорідної стовпчастої структури та показує, що розмір частинок і середньоквадратична шорсткість CZO збільшуються зі збільшенням товщини. УФ-видима спектроскопія показує (у видимій області) пропускання від 75 до 86 % для всіх плівок, сильне поглинання (в УФ-області) і зменшення оптичної забороненої зони. Крім того, товщина впливає на ближній край смуги (NBE) і видиме випромінювання, що виявляється фотолюмінесценцією. Електропровідність зразка з довжиною хвилі 725 нм становить  $4,43 \text{ (Ом}\cdot\text{см)}^{-1}$ .

**Ключові слова:** Тонкі плівки ZnO, леговані Co; Покриття зануренням; Товщина, Фотолюмінесценція, XRD, Електропровідність.